PHYSICAL REVIEW D VOLUME 43, NUMBER 5 1 MARCH 1991

Properties of P-wave mesons with one heavy quark

Stephen Godfrey*
Guelph-Waterloo Program for Graduate Work in Physics, Department of Physics, University of Guelph, Guelph, Canada N1G 2W1

Richard Kokoski
Department of Physics, University of Toronto, Toronto, Canada M5S 1A7
(Received 14 August 1990)

We present the results of a quark model study of $L=1$ mesons with one heavy quark. We give the masses of these states as predicted by the relativized quark model and the decay properties as calculated using both the pseudoscalar emission model and the flux-tube-breaking model. We examine the idealized limit of one infinitely massive quark and one light quark and discuss our results in this context as a guide to what can be learned from the study of these states. We find that, even for B mesons, the tensor interactions play an important role in the spectroscopy and the $m_Q \rightarrow \infty$ has not yet been reached. We conclude that further experimental study of the decay properties of the D_1 mesons is important to the understanding of the ${}^3P_1$-${}^1P_1$ mixing mechanism.

I. INTRODUCTION

Quark models have achieved considerable success in describing hadron properties,[1] and although it is becoming increasingly clear that the quark model is a reasonable approximation to QCD in the hadron sector,[2] it is always useful to test models in new situations. One such laboratory is the study of mesons which contain one heavy quark such as the charmed and beauty mesons.[3,4] These systems are especially interesting because, as pointed out by De Rújula, Georgi, and Glashow,[3] as the heavy quark's mass increases, its motion decreases, and so the meson's properties will increasingly be governed by the dynamics of the light quark and will approach a universal limit. As such, these states become the hydrogen atoms of hadron physics. For the P-wave mesons the light quark's spin couples with the orbital angular momentum, resulting in two degenerate $j=\frac{3}{2}$ states, the 2^+ and 1^+ states, and two degenerate $j=\frac{1}{2}$ states, the 0^+ and the other 1^+ state. With the observation of excited charmed mesons by the ARGUS,[5] CLEO,[6] and Fermilab E691 (Ref. 7) Collaborations, and the prospect of observing more such states, further study of these states is timely. In this paper we discuss the properties of the P-wave mesons with one heavy quark.[8,9] Our goal is to present the results of a specific model as a guide to interpreting experimental data and to discuss the physics that can be learned from the study of these states.

The model on which the mass predictions are based is a relativized version of the usual quark potential model which includes one-gluon exchange with a running coupling constant and a linear confining potential.[10,11] The main features of the model are its use of relativistic kinematics and of momentum-dependent and nonlocal interactions. With only a few free parameters, the model leads to a reasonable description of all known mesons[10,11] and baryons.[12] The model has also been subjected to an extensive test of its ability to predict weak, electromagnetic, and strong couplings of mesons. The strong decay analysis was originally performed using an elementary pseudoscalar emission model,[10] but has more recently been extended with the use of a QCD-motivated flux-tube-breaking decay model.[13] The latter, more fundamental approach allows us to predict decay rates to all possible Okubo-Zweig-Iizuka- (OZI-)rule-allowed final states in terms of just one parameter. In view of the success of these models in describing known meson properties, we believe that they provide a reasonable description of meson structure.

We begin in Sec. II with a brief description of the relativized quark model and its predictions for meson masses and ${}^3P_1$-${}^1P_1$ mixing. In Sec. III we study the decay properties of these states first using the pseudoscalar emission model and then the flux-tube-breaking decay model to compare the results and gauge the accuracy of our predictions. In Sec. IV we turn to a simplified analysis of the P-wave mesons to help interpret our results and comment on what the study of P-wave mesons will teach us about the nature of the interquark potential. We relate our results to experimental observations in Sec. V and summarize our main conclusions in Sec. VI.

II. MASS PREDICTIONS

To include relativistic effects, Ref. 10 did not carry out a relativization from first principles, but rather constructed a quark potential motivated by the expected relativistic properties. Mesons were approximated by the $q\bar{q}$ sector of Fock space, in effect, integrating out the degrees of freedom below some distance scale μ^{-1}. This resulted in an effective potential $V(\mathbf{p},\mathbf{r})$, whose dynamics are governed by a Lorentz-vector one-gluon-exchange interaction at short distances and a Lorentz-scalar linear confining interaction. The basic equation of the model is the rest-frame Schrödinger-type equation

$$H|\psi\rangle=[H_0+V_{q\bar{q}}(\mathbf{p},\mathbf{r})]|\psi\rangle=E|\psi\rangle \ , \tag{1}$$

where

$$H_0=(p^2+m_q^2)^{1/2}+(p^2+m_{\bar{q}}^2)^{1/2} , \tag{2}$$

and $V_{q\bar{q}}(\mathbf{p},\mathbf{r})$ is the quark-antiquark potential, which is, because of relativistic effects, momentum dependent in addition to being coordinate dependent: $\mathbf{p}=\mathbf{p}_1=-\mathbf{p}_2$ is the center-of-mass momentum and $\mathbf{r}$ becomes the normal spatial coordinate in the nonrelativistic limit.

$V_{q\bar{q}}(\mathbf{p},\mathbf{r})$ was found by equating the scattering amplitude of free quarks, using a scattering kernel with the desired Dirac structure, with the effects between bound quarks inside a hadron.[14] To first order in $(v/c)^2$, this reduces to the standard nonrelativistic result:

$$V_{q\bar{q}}(\mathbf{p},\mathbf{r})\rightarrow V(\mathbf{r})=H_{q\bar{q}}^{\text{conf}}+H_{q\bar{q}}^{\text{cont}}+H_{q\bar{q}}^{\text{ten}}+H_{q\bar{q}}^{\text{SO}} , \tag{3}$$

where

$$H_{q\bar{q}}^{\text{conf}}=C+br+\frac{\alpha_s(r)}{r}\mathbf{F}_q\cdot\mathbf{F}_{\bar{q}} \tag{4}$$

includes the spin-independent linear confinement and Coulomb-like interaction;

$$H_{q\bar{q}}^{\text{cont}}=-\frac{8\pi}{3}\frac{\alpha_s(r)}{m_q m_{\bar{q}}}\mathbf{S}_q\cdot\mathbf{S}_{\bar{q}}\delta^3(\mathbf{r})\,\mathbf{F}_q\cdot\mathbf{F}_{\bar{q}} \tag{5}$$

is the color contact interaction;

$$H_{q\bar{q}}^{\text{ten}}=-\frac{\alpha_s(r)}{m_q m_{\bar{q}}}\frac{1}{r^3}\left[\frac{3\mathbf{S}_q\cdot\mathbf{r}\,\mathbf{S}_{\bar{q}}\cdot\mathbf{r}}{r^2}-\mathbf{S}_q\cdot\mathbf{S}_{\bar{q}}\right]\mathbf{F}_q\cdot\mathbf{F}_{\bar{q}} \tag{6}$$

is the color tensor interaction;

$$H_{q\bar{q}}^{\text{SO}}=H_{q\bar{q}}^{\text{SO(CM)}}+H_{q\bar{q}}^{\text{SO(TP)}} \tag{7}$$

is the spin-orbit interaction with

$$H_{q\bar{q}}^{\text{SO(CM)}}=-\frac{\alpha_s(r)}{r^3}\left[\frac{\mathbf{S}_q}{m_q m_{\bar{q}}}+\frac{\mathbf{S}_{\bar{q}}}{m_q m_{\bar{q}}}+\frac{\mathbf{S}_q}{m_q^2}+\frac{\mathbf{S}_{\bar{q}}}{m_{\bar{q}}^2}\right]\cdot\mathbf{L}\,\mathbf{F}_q\cdot\mathbf{F}_{\bar{q}} \tag{8}$$

its color-magnetic piece arising from one-gluon exchange; and

$$H_{q\bar{q}}^{\text{SO(TP)}}=-\frac{1}{2r}\frac{\partial H_{q\bar{q}}^{\text{conf}}}{\partial r}\left[\frac{\mathbf{S}_q}{m_q^2}+\frac{\mathbf{S}_{\bar{q}}}{m_{\bar{q}}^2}\right]\cdot\mathbf{L} \tag{9}$$

the Thomas precession term. In these formulas, $\langle \mathbf{F}_q\cdot\mathbf{F}_{\bar{q}}\rangle=-\frac{4}{3}$ for a meson and $\alpha_s(r)$ is the running coupling constant of QCD. To relativize the $q\bar{q}$ potential, the full Dirac scattering amplitude was used as a starting point from which (1) the coordinate $\mathbf{r}$ was smeared over the distances of the order of the inverse quark mass by convoluting the potential with a Gaussian form factor, and (2) factors of m_i^{-1} were replaced with, roughly speaking, factors of $(p^2+m_i^2)^{-1/2}$. The details of this *relativization* procedure and the method of solution can be found in Ref. 10.

For the case of a quark and antiquark of unequal mass, charge-conjugation parity is no longer a good quantum number, and so the $^3P_1$ and $^1P_1$ states can mix via the spin-orbit interaction or some other mechanism. Consequently, the physical $j=1$ states are linear combinations of $^3P_1$ and $^1P_1$, which we describe by the mixing

$$\begin{aligned} Q_{\text{low}}&={}^1P_1\cos\theta+{}^3P_1\sin\theta , \\ Q_{\text{high}}&=-{}^1P_1\sin\theta+{}^3P_1\cos\theta . \end{aligned} \tag{10}$$

The Hamiltonian problem was solved in Ref. 10 using the following parameters: The slope of the linear confining potential is 0.18 GeV^2, $m_u=m_d=0.22$ GeV, $m_s=0.419$ GeV, $m_c=1.628$ GeV, and $m_b=4.977$ GeV. The masses of the lowest-lying $L=0$ and 1 $s\bar{u}$, $c\bar{u}$, $c\bar{s}$, $b\bar{u}$, $b\bar{s}$ and $b\bar{c}$ mesons and the $^3P_1$-$^1P_1$ mixings are given in Table I. Some of these mesons where omitted in Ref. 10 for brevity.

III. DECAY PROPERTIES

While the mass predictions are one measure of a model's success, meson decay properties are a more sensitive test of their internal structure. To this end we examine meson decays using two different models and compare the results as an indication of their reliability.

In calculating the *P*-wave meson decays, we find that OZI-rule-allowed decays can be described by two independent amplitudes; *S* and *D* waves, which we label *S*

TABLE I. Masses and the $^3P_1$-$^1P_1$ mixing angles due to the spin-orbit interaction of Eq. (7) of the $L=1$ mesons with one heavy quark. The masses are given in GeV.

State	$s\bar{u}$ (K)	$c\bar{u}$ (D)	$c\bar{s}$ (D_s)	$b\bar{u}$ (B)	$b\bar{s}$ (B_s)	$b\bar{c}$ (B_c)
$^3P_2$	1.43	2.50	2.59	5.80	5.88	6.77
Q_{high}	1.37	2.47	2.56	5.78	5.86	6.75
Q_{low}	1.35	2.46	2.55	5.78	5.86	6.74
$^3P_0$	1.24	2.40	2.48	5.76	5.83	6.71
$^3S_1$	0.90	2.04	2.13	5.37	5.45	6.34
$^1S_0$	0.47	1.88	1.98	5.31	5.39	6.27
$^3P_1$	1.37	2.47	2.55	5.78	5.86	6.74
$^1P_1$	1.35	2.46	2.55	5.78	5.86	6.75
θ	$-5°$	$-26°$	$-38°$	$-31°$	$-40°$	$68°$

and D. For the physical $j=1$ states, since they are linear combinations of the $^3P_1$ and $^1P_1$ states, the decay amplitudes for $Q_{\rm low}$ and $Q_{\rm high}$, using the conventions of Eq. (10), are given by

$$A_S^{\bar{q}}(Q_{\rm low}\to {}^3S_1\pi)\propto \sin(\theta+\theta_0)S\ , \tag{11a}$$

$$A_D^{\bar{q}}(Q_{\rm low}\to {}^3S_1\pi)\propto \cos(\theta+\theta_0)D\ , \tag{11b}$$

$$A_S^{\bar{q}}(Q_{\rm high}\to {}^3S_1\pi)\propto \cos(\theta+\theta_0)S\ , \tag{11c}$$

$$A_D^{\bar{q}}(Q_{\rm high}\to {}^3S_1\pi)\propto -\sin(\theta+\theta_0)D\ , \tag{11d}$$

where $\sin\theta_0=\sqrt{1/3}$ and $\cos\theta_0=\sqrt{2/3}$, and so $\theta_0\simeq 35.3°$ and the subscripts S and D refer to S- and D-wave decays.

In the next two subsections, we will briefly describe how the S and D amplitudes are obtained from the pseudoscalar emission and the flux-tube-breaking models, and present our results.

A. Decays by pseudoscalar-meson emission

In this approach meson decay proceeds through a single-quark transition via the emission of a pseudoscalar meson as depicted in Fig. 1.[10] Since these amplitudes are approximations to a pair-creation amplitude, one must be careful to only include distinct pair-creation processes. We assume that the pair creation of u, d, and s quarks is approximately SU(3) symmetric. The amplitudes for pseudoscalar emission are given in Ref. 10, which, following Ref. 10, we apply by using the harmonic-oscillator wave functions of SU(6) rather than our full wave functions. This allows us to calculate the amplitudes analytically to reveal the intrinsic relations between them. The effect of this simplification is discussed in the context of the flux-tube-breaking model. The resulting amplitudes are given in terms of either the "structure-independent" D-type amplitude[15]

$$D=A_Q\left[\frac{m_Q}{m_Q+m_{\bar{q}}}\right]\left[\frac{q}{\beta}\right]^2\left[\frac{\beta}{\beta_Q}\right]\left[\frac{q}{2\pi}\right]^{1/2}F(q^2)\ , \tag{12}$$

where A_Q is given by

$$A_Q=\left[g+\frac{h}{2}\frac{m_{\bar{q}}}{m_{\bar{q}}+m_Q}\right]\beta\ , \tag{13}$$

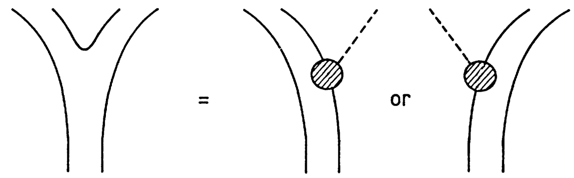

FIG. 1. Approximating meson decay amplitudes with the single-quark transition of the pseudoscalar emission model.

and $F(q^2)$ by

$$F(q^2)=\exp\left[-\left[\frac{m_Q}{m_Q+m_{\bar{q}}}\right]^2\frac{q^2}{4\beta_Q^2}\right]\ ,$$

or the "structure-dependent" S-type amplitude

$$S=S_Q\left[\frac{q}{2\pi}\right]^{1/2}F(q^2)\ , \tag{14}$$

where S_Q is given by

$$S_Q=\left[3h-\frac{A_Q}{\beta}\frac{m_Q}{m_{\bar{q}}+m_Q}\frac{q^2}{\beta_Q^2}\right]\beta_Q\ , \tag{15}$$

which has additional polynomial momentum dependences which are sensitive to the structure of the states. In these formulas, q is the momentum of the final-state mesons in the rest frame of the initial meson. Rather than calculating these various reduced amplitudes in terms of g and h, we follow Ref. 10 and use the fitted values $A_Q\simeq A=1.67$ and $S_Q\simeq S=3.27$, where A and S are the $m_Q=m_q$ limits. The harmonic-oscillator parameter β is fitted to be 0.40 GeV as in Ref. 10, while the β_Q are fitted such that the rms momenta of the harmonic-oscillator wave functions agree with values given by the relativized wave functions of Ref. 10. These are given in Table II. In Table III we give the amplitude formulas along with the numerical values for the partial widths. Note that B_c^* widths are not included since they are not OZI-rule allowed. They could decay via $B_c^*\to B_c^*\pi\pi$,

TABLE II. Meson effective β values in GeV. The *effective* β of a state is defined to be the β of the corresponding harmonic-oscillator wave function which reproduces that state's rms momentum.

State	$s\bar{u}$ (K)	$c\bar{u}$ (D)	$c\bar{s}$ (D_s)	$b\bar{u}$ (B)	$b\bar{s}$ (B_s)	$b\bar{c}$ (B_c)
$^1S_0$	0.71	0.66	0.71	0.63	0.69	1.01
$^3S_1$	0.48	0.54	0.59	0.57	0.63	0.89
$^3P_2$	0.39	0.45	0.48	0.49	0.52	0.67
$^3P_1$	0.45	0.50	0.52	0.53	0.56	0.71
$^1P_1$	0.45	0.50	0.52	0.52	0.57	0.70
$^3P_0$	0.50	0.54	0.57	0.56	0.59	0.76

where the π's come from the hadronization of the emitted gluons; however, this is beyond the scope of the present analysis.

B. Decays by flux-tube breaking

The flux-tube-breaking decay model is a variation of the quark-pair-creation (QPC) model[16] which more closely describes the actual decay processes. In the quark-pair-creation model, the elementary process is described by the creation of a $q\bar{q}$ pair with the quantum numbers of the vacuum. $J^{PC}=0^{++}$, in the final state. The initial quark and antiquark are treated as spectators, and so their momentum and spin remain unchanged. This approach results in amplitudes with all three hadrons participating in the decay treated on an equal footing. The greatest advantage of this approach is that it requires only one overall normalization constant for the pair-creation process, unlike the pseudoscalar emission model which requires many parameters. Because this model provides an accurate description of observed decays with only this one parameter, it allows us to put a high degree of confidence in its predictions. In the flux-tube-breaking model, the flux-tube-like structure of the decaying meson and its implications for the quark-pair-creation amplitudes are taken into account by viewing a meson decay as occurring via the breaking of the flux tube with the simultaneous creation of a quark-antiquark pair. To in-

TABLE III. Decay amplitudes and widths of $L=1$ mesons with one heavy quark. The amplitudes S and D are defined in the text. Our notation $A\to[BC]_L$ denotes the relative angular momentum L of B and C. γ_0 is fitted to the decay $\rho\to\pi\pi$ and is found to be $\gamma_0=0.39$ for the case of equal β's and $\gamma_0=0.78$ for the case of effective β's. The values of the constituent quark masses used in this table are $m_q=0.3$ GeV, $m_s=0.5$ GeV, $m_c=1.7$ GeV, and $m_b=5.0$ GeV. For the pseudoscalar emission model, we used the average β's: $\beta_{cq}=0.50$ GeV, $\beta_{cs}=0.53$ GeV, $\beta_{bq}=0.53$ GeV, and $\beta_{bs}=0.55$ GeV. The decays $Q_{bs}\to B^*K$ are slightly below threshold. We give the reduced amplitudes at threshold for these decays so that, if the decays are observed, one could use the correct phase space to obtain the predicted widths.

		Pseudoscalar emission model		Flux-tube model Equal β's		Flux-tube model Effective β's	
Decay	Amplitude formula	$A/q^{L+1/2}$ (GeV^{-L})	Γ (MeV)	$A/q^{L+1/2}$ (GeV^{-L})	Γ (MeV)	$A/q^{L+1/2}$ (GeV^{-L})	Γ (MeV)
$D_2^*\to D^*\pi$	$-\sqrt{3/10}D$	-1.39	19	-1.29	17	-1.18	14
$D_2^*\to D\pi$	$-\sqrt{1/15}D$	-1.03	44	-0.91	35	-0.90	23
$D_2^*\to D\eta$	$\sqrt{1/30}D$	0.49	0.25	0.52	0.27	0.38	0.14
$Q_{cH}\to[D^*\pi]_S$	$\sqrt{1/2}\cos(\theta+\theta_0)S$	0.82	250	0.86	270	1.73	1100
$Q_{cH}\to[D^*\pi]_D$	$-\sqrt{1/2}\sin(\theta+\theta_0)D$	-0.28	0.53	-0.26	0.48	-0.22	0.34
$Q_{cL}\to[D^*\pi]_S$	$\sqrt{1/2}\sin(\theta+\theta_0)S$	0.13	6.0	0.14	6.7	0.27	26
$Q_{cL}\to[D^*\pi]_D$	$\sqrt{1/2}\cos(\theta+\theta_0)D$	1.82	20	1.69	17	1.42	12
$D_0^*\to D\pi$	$-\sqrt{1/2}S$	-0.80	290	-0.61	170	-1.49	990
$D_{s2}^*\to D^*K$	$\sqrt{2/5}D$	1.50	1.0	1.79	1.4	1.56	1.0
$D_{s2}^*\to DK$	$\sqrt{4/15}D$	1.13	20	1.27	26	0.99	15
$D_{s2}^*\to F\eta$	$-\sqrt{1/15}D$	-0.61	0.26	-0.74	0.38	-0.48	0.16
$Q_{csH}\to[D^*K]_S$	$-\sqrt{2/3}\cos(\theta+\theta_0)S$	-1.05	140	-1.53	300	-2.60	860
$Q_{csH}\to[D^*K]_D$	$+\sqrt{2/3}\sin(\theta+\theta_0)D$	-0.10	~ 0	-0.12	~ 0	-0.10	~ 0
$Q_{csL}\to[D^*K]_S$	$-\sqrt{2/3}\sin(\theta+\theta_0)S$	0.053	0.31	0.08	0.64	0.13	1.82
$Q_{csL}\to[D^*K]_D$	$-\sqrt{2/3}\cos(\theta+\theta_0)D$	-2.01	0.05	-2.4	0.07	1.90	0.04
$D_{s0}^*\to DK$	$\sqrt{2/3}S$	1.02	310	0.95	270	1.83	990
$D_{s0}^*\to F\eta$	$-\sqrt{1/6}S$			Below Threshold			
$B_2^*\to B^*\pi$	$-\sqrt{3/10}D$	-1.44	19	-1.34	17	-1.16	13
$B_2^*\to B\pi$	$-\sqrt{1/5}D$	-1.13	23	-1.02	19	-0.85	14
$Q_{bH}\to[B^*\pi]_S$	$\sqrt{1/2}\cos(\theta+\theta_0)S$	0.82	250	0.88	290	1.84	1300
$Q_{bH}\to[B^*\pi]_D$	$-\sqrt{1/2}\sin(\theta+\theta_0)D$	-0.14	0.15	-0.13	0.13	-0.09	0.07
$Q_{bL}\to[B^*\pi]_S$	$\sqrt{1/2}\sin(\theta+\theta_0)S$	0.06	1.2	0.07	1.6	0.14	7.3
$Q_{bL}\to[B^*\pi]_D$	$\sqrt{1/2}\cos(\theta+\theta_0)D$	1.90	25	1.77	22	1.43	14
$B_0^*\to B\pi$	$-\sqrt{1/2}S$	-0.81	270	-0.69	200	-1.58	1000
$B_{s2}^*\to B^*K$	$\sqrt{2/5}D$	1.73	0.07	2.04	0.08	1.59	0.05
$B_{s2}^*\to BK$	$\sqrt{4/15}D$	1.35	2.6	1.55	3.3	1.17	1.9
$Q_{bsH}\to[B^*K]_S$	$-\sqrt{2/3}\cos(\theta+\theta_0)S$	-1.06		-1.6		-2.7	
$Q_{bsH}\to[B^*K]_D$	$+\sqrt{2/3}\sin(\theta+\theta_0)D$	-0.18		-0.19		-0.12	
$Q_{bsL}\to[B^*K]_S$	$-\sqrt{2/3}\sin(\theta+\theta_0)S$	0.088		0.12		0.20	
$Q_{bsL}\to[B^*K]_D$	$-\sqrt{2/3}\cos(\theta+\theta_0)D$	-2.20		-2.5		-1.7	
$B_{s0}^*\to BK$	$\sqrt{2/3}S$	1.04	170	1.21	220	2.05	630

corporate this into the QPC model, the pair creation amplitude γ is allowed to vary in space so that the $q\bar{q}$ pair is produced within the confines of a flux-tube-like region surrounding the initial quark and antiquark. The details of the model are described in Ref. 13.

The amplitudes are evaluated here for the limit in which γ is constant, which was shown to correspond to the usual $^3P_0$ model. This was done since it was found in Ref. 13 that the flux-tube-breaking model gives results which are very similar to the naive quark-pair-creation model, and this limit has the advantage that analytic expressions can be obtained when harmonic-oscillator wave functions are used. In this limit the S and D amplitudes are given in Ref. 13, which we reproduce here for convenience:

$$S=\sqrt{12}\left[1-\frac{q^2}{4\beta^2}(1-\xi_{qQ})(1+\xi_{qQ})\right]F_{qQ}(q^2)A\ , \tag{16}$$

and

$$D=\left[\frac{3}{4}\right]^{1/2}\frac{q^2}{\beta^2}(1+\xi_{qQ})(1-\xi_{qQ})F_{qQ}(q^2)A\ , \tag{17}$$

where

$$F_{qQ}(q^2)=\exp\left[-\frac{q^2}{12}\left[\frac{\beta^2[\beta_C^2(1+\Delta_{qQ})^2+\beta_B^2+\Delta_{qQ}^2\beta_A^2]}{2\beta_A^2\beta_B^2\beta_C^2}\right]\right]\ , \tag{18}$$

$$A=\frac{8\gamma_0\pi^{3/4}}{9\beta^{1/2}}\left[\frac{\beta}{\beta_A}\right]^{5/2}\left[\frac{\beta^2}{\beta_B\beta_C}\right]^{3/2}\left[\frac{q}{\pi}\right]^{1/2}\left[\frac{\tilde{M}_B\tilde{M}_C}{\tilde{M}_A}\right]^{1/2}\ , \tag{19}$$

$$\beta^{-2}=\tfrac{1}{3}(\beta_A^{-2}+\beta_B^{-2}+\beta_C^{-2})\ , \tag{20}$$

$$\xi_{qQ}=\frac{\beta^2}{3\beta_A^2}\left[1-\Delta_{qQ}\frac{\beta_A^2}{\beta_B^2}\right]\ , \tag{21}$$

and

$$\Delta_{qQ}=\frac{m_q-M_Q}{m_q+M_Q}\ . \tag{22}$$

The mock-meson masses $\tilde{M}_i$ are the calculated masses of the mesons in the spin-independent potential.

In evaluating Eqs. (16) and (17) to calculate the widths, we employed several variations to test the sensitivity of our results: We varied the mass of the heavy quark and found that the results were rather insensitive to wide variations of the heavy-quark mass. We compared our results for the limit of constant γ to those of the full flux-tube model and found very similar results. Likewise, the results using the full wave functions of Ref. 10 gave similar results to those using the effective β's of Table II. The widest variation was in going from using a constant $\beta=0.4$ to using the effective β's. Since all other variations more or less fall within these two extremes, we present only those results in Table III.

C. Comments on decay analysis

We first note that the decay results are, of course, very sensitive to phase space—the partial widths are proportional to q^{2L+1}, where L is the relative angular momentum of the final-state mesons. In order to reduce the systematic error in calculating the kinematic factors, we have in all cases used the predicted masses of the $Q\bar{q}$ mesons, the rationale being that it is most likely that all masses are shifted a similar amount and the difference in masses are likely to be less sensitive to the model than the absolute masses. Clearly, this is not a totally adequate procedure, and so until the masses have been measured, we also show in Table III *reduced* amplitudes which have the $q^{L+1/2}$ factor factored out. There remains some momentum dependence in these amplitudes because of the recoil factor, but the remaining sensitivity to changes in phase space is rather small in comparison to the $q^{L+1/2}$ factor.

Given the "reduced" amplitudes, we find that the D-type amplitudes are relatively insensitive to the model, justifying their label of "structure independent." The S-type amplitudes are another story. We find that there is a reasonable agreement between the pseudoscalar emission model and flux-tube model for equal β's. However, when we use the "effective" β's which reflect more accurately the internal structure of the mesons, there is a large change in the amplitudes. As a result, we make no claims on the quantitative precision of the S-wave widths, but do stress that they will be large.

The final comment is simply to emphasize that, for the $j=1$ mesons, the partial widths are sensitive to the $^3P_1$-$^1P_1$ mixing angle. Consequently, the decay widths for these states can vary significantly with small changes in the mixing angle.

IV. DISCUSSION OF RESULTS

Our purpose in presenting these results is twofold: so that they may be used as a guide by experimentalists in interpreting their results, and to relate hadron properties to the underlying theory via an *effective* interquark interaction.[17,18] With this in mind, we analyze our results in terms of an *effective* interquark potential. We start by rewriting the nonrelativistic spin-dependent potential in a form more suitable to our present discussion and interpret it as an effective interaction. We then examine the expected meson properties in the limit $m_Q \to \infty$, which we use as a benchmark to interpret our predictions. The purpose of this exercise is to assist us in relating the experimental results to the underlying theory as they become available.

We begin by rewriting the spin-orbit Hamiltonian [Eqs. (7)–(9)] in a form more transparent for our present analysis:

$$
\begin{aligned}
H_{\mathrm{SO}} &= \frac{4}{4}\frac{\alpha_s}{r^3}\frac{\mathbf{S}\cdot\mathbf{L}}{m_q m_Q} + \frac{1}{4}\left[\frac{4}{3}\frac{\alpha_s}{r^3} - \frac{b}{r}\right]\left[\left[\frac{1}{m_q^2} + \frac{1}{m_Q^2}\right]\mathbf{S}\cdot\mathbf{L} + \left[\frac{1}{m_q^2} - \frac{1}{m_Q^2}\right]\mathbf{S}_-\cdot\mathbf{L}\right] \\
&= H_{\mathrm{SO}}^{+}\mathbf{S}\cdot\mathbf{L} + H_{\mathrm{SO}}^{-}\mathbf{S}_-\cdot\mathbf{L} \\
&= H_{\mathrm{SO}}^{q}\mathbf{S}_q\cdot\mathbf{L} + H_{\mathrm{SO}}^{Q}\mathbf{S}_Q\cdot\mathbf{L}\ ,
\end{aligned} \tag{23}
$$

where $\mathbf{S}=\mathbf{S}_q+\mathbf{S}_Q$, $\mathbf{S}_-=\mathbf{S}_q-\mathbf{S}_Q$, and the definitions of H_{SO}^{q} and H_{SO}^{Q} follow from Eq. (23). With this Hamiltonian, we obtain the following mass formulas for the P-wave mesons:

$$M(^3P_2) = M_0 + \tfrac{1}{4}\langle H_{\mathrm{cont}}\rangle - \tfrac{1}{10}\langle H_{\mathrm{ten}}\rangle + \langle H_{\mathrm{SO}}^{+}\rangle\ , \tag{24a}$$

$$\begin{bmatrix} M(^3P_1) \\ M(^1P_1) \end{bmatrix} = \begin{bmatrix} M_0 + \tfrac{1}{4}\langle H_{\mathrm{cont}}\rangle + \tfrac{1}{2}\langle H_{\mathrm{ten}}\rangle - \langle H_{\mathrm{SO}}^{+}\rangle & -\sqrt{2}\langle H_{\mathrm{SO}}^{-}\rangle \\ -\sqrt{2}\langle H_{\mathrm{SO}}^{-}\rangle & M_0 - \tfrac{3}{4}\langle H_{\mathrm{cont}}\rangle \end{bmatrix} \begin{bmatrix} ^3P_1 \\ ^1P_1 \end{bmatrix}\ , \tag{24b}$$

$$M(^3P_0) = M_0 + \tfrac{1}{4}\langle H_{\mathrm{cont}}\rangle - \langle H_{\mathrm{ten}}\rangle - 2\langle H_{\mathrm{SO}}^{+}\rangle\ , \tag{24c}$$

where the $\langle H_i\rangle$ are the expectation values of the spatial parts of the various terms, M_0 is the center of mass of the multiplet, and we have adopted a phase convention corresponding to the order of coupling $\mathbf{L}\times\mathbf{S}_Q\times\mathbf{S}_q$.

To put our model's results into context, we start by studying the limit where $m_Q \to \infty$ in which the mass formulas simplify to

$$M(^3P_2) = M_0 + \langle H_{\mathrm{SO}}^{q}\rangle\ , \tag{25a}$$

$$\begin{bmatrix} M(^3P_1) \\ M(^1P_1) \end{bmatrix} = \begin{bmatrix} M_0 - \langle H_{\mathrm{SO}}^{q}\rangle & -\sqrt{2}\langle H_{\mathrm{SO}}^{q}\rangle \\ -\sqrt{2}\langle H_{\mathrm{SO}}^{q}\rangle & M_0 \end{bmatrix} \begin{bmatrix} ^3P_1 \\ ^1P_1 \end{bmatrix}\ , \tag{25b}$$

$$M(^3P_0) = M_0 - 2\langle H_{\mathrm{SO}}^{q}\rangle\ . \tag{25c}$$

One first notes that in this limit, for $\langle H_{\mathrm{SO}}^{q}\rangle$ positive, the $^3P_1$ state starts out with lower mass than the $^1P_1$ state, and so after mixing the lower state will be predominantly $^3P_1$. Using the definition of Eq. (10), we find that $\sin\theta=\sqrt{2/3}$ and $\cos\theta=\sqrt{1/3}$, resulting in the masses $M_{\mathrm{low}}=M_0-2\langle H_{\mathrm{SO}}^{q}\rangle$ and $M_{\mathrm{high}}=M_0+\langle H_{\mathrm{SO}}^{q}\rangle$. For the case of $\langle H_{\mathrm{SO}}^{q}\rangle$ negative the level ordering of the $^3P_2$ and $^3P_0$ invert [i.e., $M(^3P_0)>M(^3P_2)$] and the $^3P_1$ state starts out with higher mass than the $^1P_1$ state, and so after mixing the lower state is predominantly $^1P_1$. Here $\sin\theta=-\sqrt{1/3}$ and $\cos\theta=\sqrt{2/3}$ with $M_{\mathrm{low}}=M_0+\langle H_{\mathrm{SO}}^{q}\rangle$ and $M_{\mathrm{high}}=M_0-2\langle H_{\mathrm{SO}}^{q}\rangle$. Thus, for both cases, in the $m_Q\to\infty$ limit, the state degenerate with the $^3P_2$ will be mainly $^1P_1$ and the state degenerate with the $^3P_0$ will be mainly $^3P_1$.

To actually measure the $^3P_1$-$^1P_1$ mixing angle and learn more about the interquark potential, we turn to the decays. From Eq. (11) the widths are given by

$$\Gamma(Q_{\mathrm{low}}\to {}^3S_1\pi) \propto [S^2\sin^2(\theta+\theta_0)+D^2\cos^2(\theta+\theta_0)]\ , \tag{26a}$$

$$\Gamma(Q_{\mathrm{high}}\to {}^3S_1\pi) \propto [S^2\cos^2(\theta+\theta_0)+D^2\sin^2(\theta+\theta_0)]\ , \tag{26b}$$

so that in the limit $m_Q\to\infty$ we find that for both positive and negative $\langle H_{\mathrm{SO}}^{q}\rangle$ the state degenerate with the $^3P_0$ is purely S wave and the state degenerate with the $^3P_2$ is purely D wave. Thus, by measuring the angular distribution of the decay products, one can obtain an estimate of the $^3P_1$-$^1P_1$ mixing angle and hence the sign and magnitude of the mixing amplitude which can be related to that of the spin-orbit part of the potential.

Of course, the physical situation will be more complicated, and so with this in mind, we analyze the predictions of our model as an exercise in extracting the *effective* spin-dependent potentials for the different meson families. As a first step, we neglect the off-diagonal mixing term and study the unmixed $^3P_1$ and $^1P_1$ masses. Solving for $\langle H_i\rangle$, we obtain the values quoted in Table IV. One finds, at least in our model, that the contact and tensor terms are not negligible for any flavor family of mesons. In fact, not even for the B mesons does the $^3P_1$-$^1P_1$ inversion occur. This may seem unexpected, but recall that, in the relativized model, the quark masses in the spin-dependent potentials are replaced by roughly $\langle E_q\rangle \simeq (m_q^2+\langle p^2\rangle)^{1/2}\simeq\sqrt{2m_q}$ since, for light-quark systems, $m_q\simeq\langle p^2\rangle\simeq\Lambda_{\mathrm{QCD}}$, the only available scale in QCD. Thus the effect of increasing the quark mass is not nearly as big as expected from the nonrelativistic quark model. In general, one does note that the contact and tensor terms decrease in magnitude as the quark masses increase; the one exception is going from $b\bar{u}\to b\bar{s}\to b\bar{c}$. This small deviation from the general pattern is explained

TABLE IV. Expectation values of the spin-dependent effective potentials for $L=1$ mesons with unequal mass quarks as predicted by the relativized model of Ref. 10. The first row gives the values of the reduced mass μ of the $Q\bar{q}$ pair in the mesons. All values are given in MeV.

State	$s\bar{u}$ (K)	$c\bar{u}$ (D)	$c\bar{s}$ (D_s)	$b\bar{u}$ (B)	$b\bar{s}$ (B_s)	$b\bar{c}$ (B_c)
μ	188	255	386	283	454	1270
M_0	1378	2474	2564	2786	5864	6752
$\langle H_{\rm cont}\rangle$	33	20	15	8	7	4
$\langle H_{\rm SO}^{+}\rangle$	47	26	27	10	11	17
$\langle H_{\rm ten}\rangle$	56	27	28	11	12	14

by the fact that, with a larger reduced mass, the wave function will become more compact, increasing the value of $\langle r^{-3}\rangle$. A final comment regards the noninversion of the $^3P_1$-$^1P_1$ pair. For this to occur requires that $\langle H_{\rm SO}^{+}\rangle > \langle \frac{1}{2}H_{\rm ten}+H_{\rm cont}\rangle$, which only occurs for the $b\bar{c}$ system, demonstrating that if and when such multiplet inversion occurs will give us some insight into the importance of relativistic effects in hadron spectroscopy.

We now proceed to include the $^3P_1$-$^1P_1$ mixing term. From Eq. (8) we see that $H_{\rm SO}^{+}$ is comprised of two terms, the first of which is identical to $H_{\rm ten}$. Subtracting $\langle H_{\rm ten}\rangle$ from $\langle H_{\rm SO}^{+}\rangle$, we find that the second term of $\langle H_{\rm SO}^{+}\rangle$ is close to zero, implying that the linear, Lorentz scalar, part of the potential and the Coulomb, Lorentz vector, part of the potential are similar in importance.

To see the effect of the mixing amplitude on the mixing angle and therefore on the decay amplitudes, we show in Fig. 2 the mixing angle as a function of the mixing amplitude. We start with the unmixed $^3P_1$-$^1P_1$ $c\bar{u}$ states and plot the mixing angle as we vary the off-diagonal term in the mass matrix. Since the mixing angle is most sensitive to values of the mixing amplitude near zero, a measurement of the mixing angle could provide information about the relative importance of the Coulomb and linear pieces of the potential. To show the sensitivity of the widths to the $^3P_1$ and $^1P_1$ mixing amplitudes and mixing angles, in Fig. 3(a) we plot the partial widths as a function of the mixing amplitude and in Fig. 3(b) we plot the partial widths as a function of the mixing angle. With the mixing angles predicted by the relativized quark model, the high-mass states decay predominantly into an S wave. For the low-mass states, the S-wave partial width is suppressed, but since the S-wave amplitude is so much larger than the D-wave amplitude, the S-wave amplitude still dominates. This pattern is opposite to what we obtained in the $m_Q\rightarrow\infty$ limit. However, because the $^3P_1$ and $^1P_1$ states are nearly degenerate and the spin-orbit mixing amplitude is so small, the correct physics may not

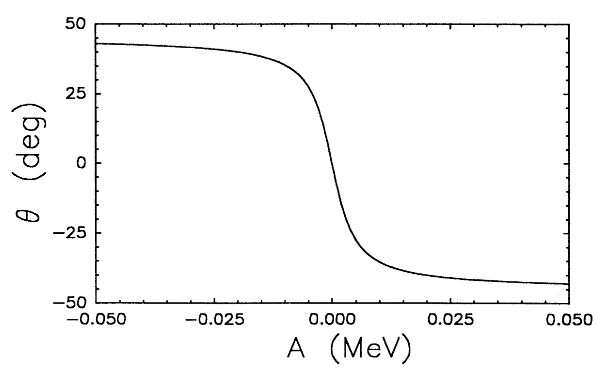

FIG. 2. $^3P_1$-$^1P_1$ mixing angle vs the mixing amplitude.

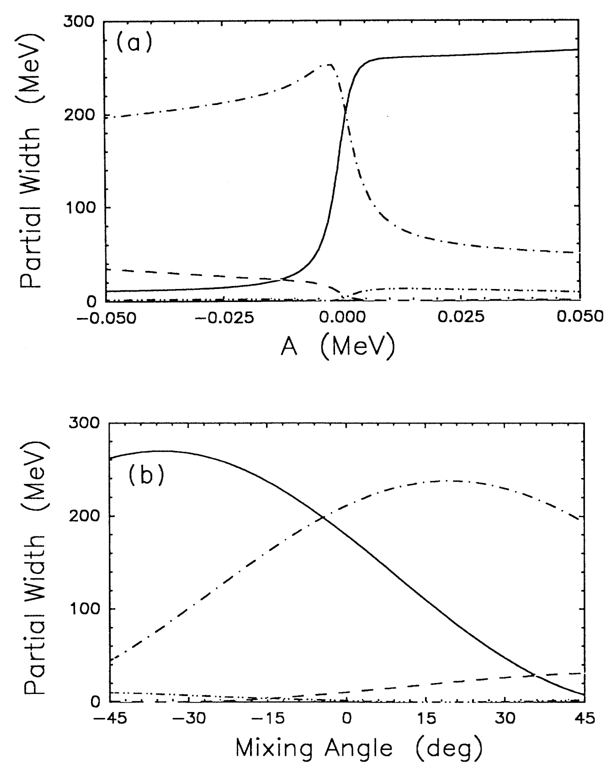

FIG. 3. $J=1$ $c\bar{q}$ partial decay widths vs (a) the $^3P_1$-$^1P_1$ mixing amplitude and (b) the $^3P_1$-$^1P_1$ mixing angle. For both cases, the solid line is the $Q_{\rm high}$ S-wave width, the dashed line is the $Q_{\rm high}$ D-wave width, the dot-dashed line is the $Q_{\rm low}$ S-wave width, and the dot-dot-dashed line is the $Q_{\rm low}$ D-wave width.

be determined by spin-orbit mixing at all, but by some other mechanism such as the effects of couplings to common decay channels.[19,20]

To summarize, we find that (at least in the relativized quark model) that the tensor and contact terms are still not negligible for the states we have studied so that the $m_Q \to \infty$ limit does not appear to be applicable for the D- and B-type mesons. The higher-mass $J=1$ state is mainly $^3P_1$ and the lower-mass $J=1$ state is mainly $^1P_1$. However, the relative widths of the upper and lower $J=1$ states are sensitive to the $^3P_1$-$^1P_1$ mixing angle, providing a means of gauging the sign and magnitude of the mixing amplitude and therefore the relative importance of the linear and Coulomb terms, or perhaps giving an indication that another mechanism contributes to the $^3P_1$-$^1P_1$ mixing.

V. COMMENTS ON THE OBSERVED D^{**} MESONS

Before concluding, we comment briefly on the observed D^{**} mesons. We summarize the observed states with their multiplet assignments in Table V. The evidence for the J^P assignments comes from the decay distribution measurements by ARGUS (Ref. 5) and CLEO,[6] which find that the state at 2.42 GeV decays essentially isotropically, while the state at 2.46 GeV is consistent with $J^P=2^+$. In addition, for the ratio $\Gamma(D^*(2.46)\to D\pi)/\Gamma(D^*(2.46)\to D^*\pi)$ CLEO obtains 2.3 ± 0.8 and ARGUS $3.0\pm1.1\pm1.5$, which are consistent with the theoretical prediction of ~ 2 for the $J^P=2^+$ state. On the other hand, CLEO finds the limit $\Gamma(D^*(2.42)\to D\pi)/\Gamma(D^*(2.42)\to D^*\pi)<0.24$ at 90% C.L., which is inconsistent with the 2^+ prediction. Finally, the D_0^* cannot decay to $D^*\pi$ by angular momentum and parity considerations. Although our predicted masses are slightly higher than the observed masses, the D^{**}-D^* splittings are consistent within the experimental and theoretical uncertainties.

The predicted widths for $^3P_2$ are also consistent with the observed $D^*(2.46)$ widths within the uncertainties. For the mixing angles predicted by the relativized quark model, the width of $D^*(2.42)$ is consistent with the lower $J=1$ state, although the decay analysis indicates that the decay is S wave rather than the predicted D wave for this state. However, we have previously pointed out that the decay widths are very sensitive to the mixing angle and hence the mixing amplitude. The situation is further complicated because the $J=1$ states are close enough together that they overlap and interfere. Mixing has likely caused one of the states to become narrow while the other has broadened, making it more difficult to observe. In any case, if we ignore this latter complication, from Fig. 3, if the observed state is the upper one, we would conclude that the $^3P_1$-$^1P_1$ mixing angle is positive, while if it is the lower state, the mixing angle is negative. It would be extremely useful to the understanding of these states and their mixings if more precise measurements of the decay distributions could be made so that the S- and D-wave contributions could be extracted from the total width. An additional test would be the observation of the decay $D_1\to {}^3P_0\pi\to D\pi\pi$. Since this decay is below threshold, it could only proceed because of its width, which would indicate a large component of the broad S wave. Clearly, further study of these states will add to our understanding of hadron structure.

Up to now we have restricted our comments to the observed charmed P-wave mesons. However, the CERN e^+e^- collider LEP running at $\sqrt{s}=m_Z$ will produce beauty mesons copiously. If the b quarks fragment in similar proportions as c quarks at lower energies, it may be possible to study B^{**} P-wave mesons in the near future.[21] In addition, the Collider Detector at Fermilab (CDF) Collaboration has been successful in reconstructing B mesons at the Tevatron $p\bar{p}$ collider, and so it may be possible for them to also reconstruct B^{**} mesons. Studying B^{**} will add to our understanding of the interquark interactions a little closer to the $m_Q\to\infty$ limit.

VI. SUMMARY AND CONCLUSIONS

In this paper we have presented the masses of $L=1$ mesons with one heavy quark as predicted by a relativized quark model and the decay amplitudes as predicted by the pseudoscalar emission and flux-tube-breaking models. Based on these models, we found that $\langle H_{\text{cont}}\rangle$, $\langle H_{\text{SO}}\rangle$, and $\langle H_{\text{ten}}\rangle$ all contribute to the masses of these states and cannot *a priori* be neglected if we are to understand the properties of the P-wave mesons. Thus, deter-

TABLE V. Summary of the observed D^{**} meson properties.

	ARGUS (Ref. 5)		CLEO (Ref. 6)		E691 (Ref. 7)	
	Mass (MeV)	Width (MeV)	Mass (MeV)	Width (MeV)	Mass (MeV)	Width (MeV)
$D_2^*\to D^+\pi^-$	$2455\pm3\pm5$	15^{+13+5}_{-10-10}	$2461\pm3\pm1$	$20^{+9}_{-12}{}^{+9}_{-10}$	$2459\pm3\pm8$	$21^{+12}_{-8}\pm15$
$D_2^*\to D^0\pi^+$	$2469\pm4\pm6$	$14\pm5\pm8$				
$D_1\to D^{*+}\pi^-$	2419 ± 6	41^{+22}_{-14}	$2428\pm3\pm2$	23^{+8+10}_{-6-4}	$2428\pm8\pm5$	$58\pm4\pm10$
$D_1\to D^{*0}\pi^+$	$2415\pm7\pm5$	$20\pm8\pm15$			$2443\pm7\pm5$	$41\pm19\pm8$
$D_S^{**}\to D^{*+}K^0$	$2535.9\pm0.9\pm2$	<4.6 [a]	$2535.6\pm0.7\pm0.4$	<5.44 [a]		

[a]90% C.L.

mining the level ordering of the states by measuring the masses and quantum numbers is important. Given the masses of these states, the decay properties, especially those of the $j=1$ states, will give further information about the sign and strength of the $^3P_1$-$^1P_1$ mixing amplitude to which the spin-orbit piece of the Hamiltonian contributes, which in turn could give information on the range of the Lorentz-vector piece of the potential or point to decay channel couplings as the mixing mechanism. The implications of this latter mechanism is presently under study.[20] Taken as a whole, the study of P-wave mesons will (1) give us information about the relative strength of the linear and Coulomb pieces of the potential and (2) give us information about the relative strengths of the contact, tensor, and spin-orbit pieces of the Hamiltonian, which will help us gauge the importance of relativistic effects in hadrons. As such, the study of $L=1$ mesons will add to our understanding of the nature of confinement and help refine the quark model.

ACKNOWLEDGMENTS

Interest in this subject was kindled by a review by Jonathan Rosner, but it came to fruition through the insistence of our experimental colleagues in the ARGUS and Fermilab E691 Collaborations on the usefulness of such an analysis. The authors gratefully acknowledge helpful comments by Nathan Isgur and Rob Kutschke and useful conversations with Jim Prentice. S.G. thanks TRIUMF, the Department of Physics at the University of Toronto, and Brookhaven National Laboratory for their hospitality where some of this work took place. This work was supported in part by the Natural Sciences and Engineering Research Council of Canada.

*Present address: Ottawa-Carleton Institute for Physics, Department of Physics, Carleton University, Ottawa, Canada K1S 5B6.

[1]S. Godfrey, Nuovo Cimento A **102**, 1 (1989); N. Isgur, in *Particles and Fields—1981,* edited by C. Heusch and W. T. Kirk (AIP Conf. Proc. No. 81) (AIP, New York, 1982), p. 1; J. L. Rosner, in *Techniques and Concepts of High Energy Physics,* proceedings of the NATO Advance Study Institute, St. Croix, U.S. Virgin Islands, 1980, edited by T. Ferbel (NATO ASI, Series B: Physics, Vol. 66) (Plenum, New York, 1984).

[2]S. Capstick, S. Godfrey, N. Isgur, and J. Paton, Phys. Lett. B **175**, 457 (1986).

[3]This was first pointed out by A. De Rújula, H. Georgi, and S. L. Glashow, Phys. Rev. Lett. **37**, 785 (1976).

[4]For a recent review of this subject, see J. Rosner, Comments Nucl. Part. Phys. **16**, 109 (1986).

[5]The ARGUS Collaboration, H. Albrecht *et al.*, Phys. Lett. B **221**, 422 (1989); Phys. Rev. Lett. **56**, 549 (1986); Phys. Lett. B **230**, 162 (1989); **232**, 398 (1989).

[6]The CLEO Collaboration, P. Avery *et al.*, Phys. Rev. D **41**, 774 (1990).

[7]The E691 Collaboration, J. C. Aujos *et al.*, Phys. Rev. Lett. **62**, 1717 (1989).

[8]An earlier version of this paper appeared as S. Godfrey and R. Kokoski, TRIUMF Report No. TRI-PP-86-51, 1986 (unpublished).

[9]An incomplete list of other work describing P-wave mesons in the quark model is J. Morishita *et al.*, Phys. Rev. D **37**, 159 (1988); V. Gupta and R. Kögeler, Z. Phys. C **41**, 277 (1988); R. Barbieri *et al.*, Nucl. Phys. **B105**, 125 (1976); D. Pignon and C. A. Piketty, Phys. Lett. **81B**, 334 (1979); E. Eichten *et al.*, Phys. Rev. D **21**, 203 (1980); A. Martin, Phys. Lett. B **223**, 103 (1989); D. B. Lichtenberg, R. Roncaglia, J. G. Willis, and E. Predazzi, Indiana University Report No. IUHET 175, 1989 (unpublished).

[10]S. Godfrey and N. Isgur, Phys. Rev. D **32**, 189 (1985).

[11]S. Godfrey, Phys. Rev. D **31**, 2375 (1985); S. Godfrey and N. Isgur, *ibid.* **34**, 899 (1986).

[12]S. Capstick and N. Isgur, Phys. Rev. D **34**, 2809 (1986).

[13]R. Kokoski and N. Isgur, Phys. Rev. D **35**, 907 (1987).

[14]D. Gromes, in *The Quark Structure of Matter,* proceedings of the Yukon Advanced Study Institute, Yukon, Canada 1984, edited by N. Isgur, G. Karl, and P. J. O'Donnell (World Scientific, Singapore, 1985).

[15]We use the convention of a heavy quark and a light antiquark, and the decay amplitudes are given by pseudoscalar emission from the light antiquark.

[16]A. Le Yaouanc, L. Oliver, O. Péne, and J. C. Raynal, Phys. Rev. D **8**, 2223 (1973); **9**, 1415 (1974); **11**, 1272 (1975); M. Chaichian and R. Kokerler, Ann. Phys. (N.Y.) **124**, 61 (1980).

[17]H. Schnitzer, Phys. Lett. B **226**, 171 (1989).

[18]For other examples of this approach, see S. Godfrey, Phys. Lett. B **162B**, 367 (1985); H. Schnitzer, *ibid.* **134B**, 2153 (1984); **149B**, 408 (1984); Nucl. Phys. **B207**, 131 (1983).

[19]If two states are degenerate and are then coupled to a common decay channel, they will mix to the point where one of them exactly decouples from that channel. H. J. Lipkin, Phys. Lett. **72B**, 249 (1977).

[20]S. Godfrey and N. Isgur (unpublished).

[21]P. Estabrooks (personal communication).